

## Development of a coupling technique between RELAP5 and SIMMER-IV for fusion reactor applications

Francesco Galleni<sup>a,\*</sup>, Vittorio Cossu<sup>a</sup>, Alessio Pesetti<sup>a</sup>, Marica Eboli<sup>b</sup>, Alessandro Del Nevo<sup>b</sup>, Nicola Forgone<sup>a</sup>

<sup>a</sup> University of Pisa, LSTN, DICL, Largo Lucio Lazzarino, 56122 Pisa, Italy

<sup>b</sup> ENEA FSN-ING C.R. Brasimone, 40032 Camugnano (Bo), Italy

### ARTICLE INFO

#### Keywords:

Codes coupling  
SIMMER-IV code  
RELAP5 code  
WCLL-BB  
PbLi  
Lifus5/Mod3

### ABSTRACT

A critical problem in the Water-Cooled Lead-Lithium Breeding Blanket system (WCLL-BB) is the possible interaction between the water and the Lithium-Lead eutectic alloy - which act respectively as primary coolant and as breeder/neutron multiplier - due to a postulated rupture of the coolant circuit in the Breeding Unit of the BB. This scenario involves a complex multiphase interaction together with an exothermal chemical reaction between the two fluids with the production of hydrogen.

The PbLi/water chemical reaction was implemented in SIMMER-IV code by the University of Pisa and, consequently, a coupling methodology was successfully developed between SIMMER-IV and RELAP5/Mod3.3 codes, in order to overcome SIMMER-IV unsuitability in the simulations of complex pipelines.

This paper presents an application of the coupling methodology to the simulation of experimental tests, recently performed at ENEA inside the experimental campaign carried out with the LIFUSS/Mod3 facility at the ENEA Brasimone Research Centre. The injection line of the facility is simulated by RELAP5/Mod3.3, whilst the reaction vessel is simulated with SIMMER-IV.

Results of different simulations are presented and compared against experimental data, providing both qualitative and quantitative evaluations of the performance of the coupling methodology in the prediction of the chemical and thermal-hydraulic phenomena involved in the experiments, such as the fast pressurisation of the injection line and the pressurisation of the reaction vessel, the energy release due to the chemical reaction and the propagation of pressure waves inside the reaction vessel.

### 1. Introduction and background

The development of coupling techniques to exploit distinctive features of diverse codes has been gaining more and more importance and pace in recent years. The combination of different codes can be of crucial assistance in the simulation of phenomena involving several scales, multiphase transients, chemical and thermophysical interactions, among many other applications [1–5]. In the fields concerning nuclear fusion a remarkable example of a problem which entails all these aspects is the in-box LOCA (Loss of Coolant Accident) incidental scenario, postulated to happen in the Water-Cooled Lithium-Lead Breeding Blanket configuration (WCLL-BB) [6–9]. In this scenario the Breeding Blanket coolant (i.e., liquid water), may abruptly interact with Lithium-Lead, a liquid metal eutectic alloy used as breeder and neutron multiplier. This interaction implies changes of phase, with the water

rapidly vaporizing, turbulent fluid dynamics interchanges between the multiple fluids and a chemical reaction between the Lithium and the water, both in liquid and in vapour form [10–13]. Besides these phenomena, the difficulty of the prediction and simulation of this scenario is strongly increased by the complexity of the geometries involved (the Breeding Blanket structures connected with its ancillary circuits [14–16]) and the necessity of simulating control systems which should intervene in case of accident.

Given this background, it is understandable the primary importance implied by the development of a qualified code for the evaluation of the accidental consequences and for choosing possible mitigating countermeasures, besides proposing design solutions to prevent damages to the blanket box structures. However, there are no single codes capable of efficiently and accurately handling all the aspects listed above. Therefore, in the framework of the development of the European DEMO nuclear fusion reactor and the ITER experimental reactor, several tasks

\* Corresponding author.

E-mail address: [francesco.galleni@unipi.it](mailto:francesco.galleni@unipi.it) (F. Galleni).

## Abbreviations

Abbreviation	Definition
BB	Breeding Blanket
BC	Boundary conditions
DEMO	DEMONstration Fusion Power Plant
ITER	International Thermonuclear Experimental Reactor
L5M3	LIFUS5/MOD3
LOCA	Loss of Coolant Accident
S-III	SIMMER-III
S-IV	SIMMER-IV
WCLL	Water-Cooled Lithium Lead

were dedicated to the experimental investigation of this scenario and support the creation of this numerical tool through the coupling of two different codes, namely SIMMER and RELAP5/Mod3.3 [7,17,18].

The strength of this tool is the possibility of obtaining high-fidelity calculations in complex geometries, considering multiple physical phenomena and minimizing the computational cost. On the one hand, the local interaction (i.e., the in-box accident) is simulated by SIMMER, which is a multidimensional code, capable of simulating multifluid systems, involving also solid structures and phase changes [19,20]. On the other hand, the connected loops and the control system are simulated by RELAP5, which is a well-known and well-established STH code (STH—System Thermal Hydraulics codes) in the nuclear safety analysis field [21]. Moreover, SIMMER capabilities were further increased by the University of Pisa by adding the possibility of simulating Lithium-Lead and water chemical interaction, through the exploitation of a module originally implemented to simulate the chemical reaction between Sodium and water [22]. Several studies are ongoing to test, verify and validate this implementation.

There are currently two versions of SIMMER, namely SIMMER-III and SIMMER-IV, with the first one being limited to two-dimensional axisymmetric geometries and the second one being fully three-dimensional. This paper presents the work carried out to develop, test and validate the coupling technique between SIMMER-IV and RELAP5; this technique was already successfully applied to SIMMER-III [18], but it had not been extended to SIMMER-IV until now. This work represents a crucial step forward in creating the coupling tool mentioned above, because it extends its capability to considerably more complex 3D geometries.

More in detail, the developed coupling technique can be defined as a “two-way”, “nonoverlapping”, “online” methodology [5], with the SIMMER and RELAP5 computational domains separated by interfaces and linked by an external script. Through these interfaces, data are exchanged at each time-step between the two codes in both directions in order to provide proper boundary conditions for the advancement of the calculations. The synchronized advancement in the time domain is controlled by means of an implicit coupling methodology.

The largest part of the work concerned the improvement, upgrade and adaptation of the MATLAB [23] interface developed to couple RELAP5 and S-III, to better fit 1D to 3D coupling (i.e., RELAP5 to SIMMER-IV) and to better manage a large set of data during running. This last aspect was required due to the significant increase in the number of cells in the passage from S-III to S-IV, that is from two to three-dimensional meshes.

Furthermore, the coupling algorithm and control was switched to a fully implicit type in order to increase the stability and robustness of the coupling.

Besides the preliminary tests performed during the development, in order to assess the new version of the coupling with different conditions obtained from real cases, two experimental tests from the Lifus5/Mod3 experimental campaign were fully simulated and are presented here; the

two selected cases were D15 and E41 from SERIES D and SERIES E, respectively [24–27].

### 1.1. Coupling technique

As mentioned above the coupling tool between SIMMER-IV and RELAP5 codes can be classified as a “two-way”, “non-overlapping” and “online” procedure, since the computational domains of the two codes communicate by separated interfaces (i.e. text files) which are used to exchange data in both directions, with a synchronized progression in time. The interaction is managed by one single MATLAB script, which also has the role to check the “consistency” of the physical properties exchanged at the interface, together with the control of the synchronization of the time.

An implicit method was implemented as numerical scheme: in this kind of scheme each code performs the same time step several times (“inner iterations”), each time starting from the same initial conditions and time, but with updated boundary conditions, until one or more convergence criteria are satisfied. Once convergence for the single time step is reached, the coupled variables are exchanged sequentially between the two codes at the end of the time step; in other words, the results obtained in the previous time step from one code are used as new boundary conditions for the other code, which will simulate the next time step. A more detailed explanation of the implicit scheme can be found in the next section and a flow chart of the scheme is shown in Fig. 1.

The exchanged variables are different according to the direction of the coupling. This means that SIMMER-IV provides the new pressure and temperatures to RELAP5, whilst RELAP5 imposes mass flow rates and temperatures (for both liquid and gas phases) to SIMMER-IV. However, it is important to notice that in SIMMER-IV it is possible to impose only the phase velocities, therefore, in order to impose the mass flow rate, the velocity calculated by RELAP5 must be weighted through the phase volumetric fraction in the interface cells of the SIMMER-IV domain.

#### 1.1.1. Implicit scheme

The implicit solving scheme consists of two “while” loops (Fig. 1). The first is the one that simply advances the simulation from one time-step to the next one and it ends only when the full simulation is complete (“outer iterations”).

The second one controls the successful execution of the implicit iterations (“inner iterations”). The logic behind the implicit solving scheme is to repeat each macro time-step until the results of the previous and the current inner iterations are the same. Indeed, the implicit check of consistency is not performed comparing the results at the interface of the S-IV against those of RELAP5 but comparing the results of the previous iteration (of both RELAP5 and the S-IV) against those obtained at the current iteration. If the two iterations provide identical results, then the calculation moves toward the following macro time-step, otherwise a new iteration is performed using the results of the last iteration available as boundary conditions for the S-IV and RELAP5 input decks.

The exchange of data between S-IV and RELAP5 is shown in Fig. 2. Once the check for the macro time-step  $n-1$  is satisfied, the final velocities of the liquid and vapour phases obtained in RELAP5 are used to write the first S-IV input deck of the new macro time-step (constant velocity along the macro time-step). Together with the two velocities, also the pressure and temperatures of the two phases ( $P^*$  and  $T^*$  in the figure) are also employed to define the thermodynamic state of the flowing water/steam. The S-IV input deck is then executed, and the initial and final pressure and temperature ( $P$  and  $T$  in the figure) in the cell involved in the coupling are employed to write the RELAP5 input deck. These pressures and temperatures ( $P_i$ ,  $T_i$ ,  $P_f$ , and  $T_f$  in the figure) are set as conditions inside the RELAP5 TMDPVOL involved in the coupling. The RELAP5 input deck is then executed, the implicit check is performed but fails being the first iteration (no previous iterations to perform the implicit check of consistency). The initial and final phases’

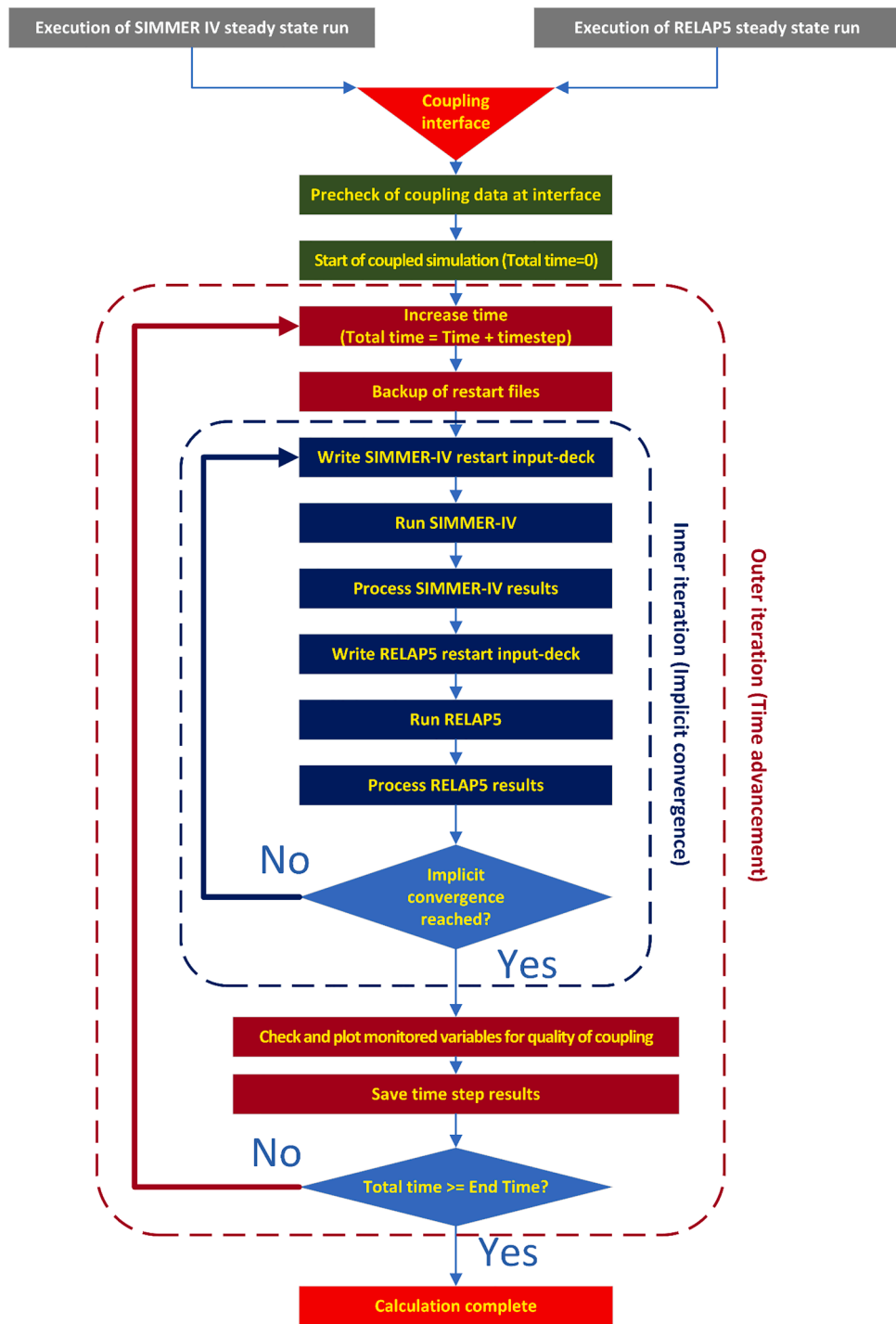


Fig. 1. SIMMER-IV / RELAP5 coupling implicit scheme.

velocities are then employed to write the new S-IV input deck for the second iteration. The S-IV input deck is then executed, and the results are employed to write the RELAP5 input deck for the second iteration... and so on until the implicit check is satisfied.

1.1.2. Multiphase coupled cells and boundary conditions

The two domains are coupled through Time dependent Volumes (TMDPVOL) in RELAP5 and boundary surfaces in S-IV.

It is important to underline that, even though the two domains are coupled imposing the BCs and hence through surfaces, the imposed values are obtained from the cells closest to the coupled surfaces. These values, however, are not calculated at boundary of the cells, but at their

centres. Therefore, in order to avoid inconsistencies in the approximation of the cell properties, the interface cells must be geometrically identical (that is having the same volumes) and relatively small.

Furthermore, whilst RELAP5 is connected through one single TMDPVOL, S-IV interface is composed of multiple surfaces/cells. This requires a slight adjustment of the coupled variables. On the one hand, the value imposed to RELAP5 is then the volume weighted average of the coupled parameters obtained from S-IV cells; it is known that this might cause some concerns about the exchanged temperatures, and this issue will certainly require further investigation. On the other hand, the situation with the BCs imposed by RELAP5 to S-IV is more complex since it involves imposing the mass flow rate. As explained above, in SIMMER-

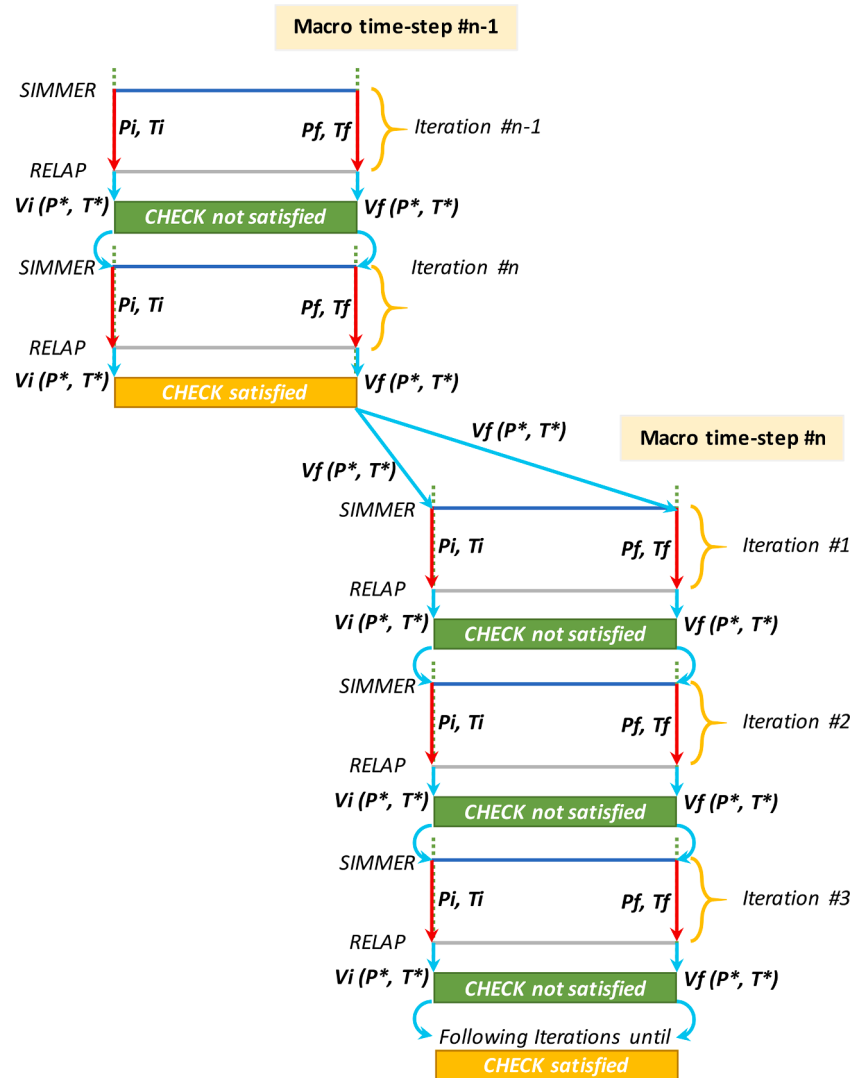


Fig. 2. Data exchange in the implicit coupling scheme.

IV it is possible to impose only the phase absolute velocities, and not the mass flow rate directly; however, in a multiphase case, the mass flow rate does not depend only on the absolute velocity of the fluid but also on the volumetric fraction. Therefore, the imposed velocity must be what is usually called the “superficial velocity”, which is calculated, in this coupling methodology, through a volume averaged value of the volumetric fractions of the phases.

Another issue that must be addressed in a coupled multiphase calculation is the appearance of one of the fluids inside the SIMMER-IV domain. As this might sound trivial, it must be recalled that in SIMMER-IV it is not possible to impose neither the volume fraction nor the mass flow rate and therefore it is not possible to insert - only by means of the BCs - new fluids inside the domains (i.e., fluids with null volume fraction at  $t = 0$ ). This concern is particularly critical for the purpose of our L5M3 test cases, where a large amount of water is suddenly inserted from RELAP5 to SIMMER, with the SIMMER-IV domain being void of water from the beginning of the calculation. This issue was addressed exploiting one feature of SIMMER-IV that was originally developed for the chemical module, the so called MASSOD option. This feature allows the user to force the code to insert a specified amount (in mass) of coolant fluid (that is, sodium or water, in SIMMER) inside selected cells (up to 40) at any time in the calculation. Therefore, the Matlab script, at the beginning of each time step, checks the mass of water inside the RELAP5 interface cell. If the mass of water is above a certain threshold,

the MASSOD option is activated in the SIMMER-IV restart file at that specific time. Since SIMMER-IV interface is composed of various cells, which might be of different volumes, a different mass of water is distributed in each cell depending on its volume, obviously maintaining the total mass of water consistent with the one calculated from RELAP5. This operation might need to be repeated a few times during the first injection since the two codes require some time steps to properly synchronise the total mass.

It must be stressed that the procedure described above, even though it was proved quite reliable, it is by no means the same as imposing boundary conditions, from a numerical point of view. This sudden appearance of mass can have a strong impact on the stability of the calculation and therefore it requires some degree of caution in choosing the time step when the option is activated.

### 1.1.3. Multiphase properties approach

Since the codes are dealing with multiple phases, in addition to the basic information exchanged in conventional liquid single-phase coupling (liquid temperature and pressure), in this multiphase coupling the two codes have to share data also on the non-condensable fluid and vapours which compose the gas phase: these data include the gas velocity and the gas mixture temperature.

In order to avoid inconsistencies in the physical properties, this gas-phase coupling was developed as one-way coupling, i.e., the properties



of the mixture at the interface are always calculated by SIMMER-IV using data from RELAP5 and no other exchange is done. The scheme for the calculation of the gas mixture properties is shown in Fig. 3. RELAP5 communicates the total pressure (PTOT), the gas temperature (TGAS) and the liquid temperature (TLIQ) to SIMMER-IV which calculates the vapour pressure (PVAP) from TLIQ. Then PVAP is assumed as the partial pressure of the vapour in the gas mixture and the partial pressure of the incondensable gas (PINC) is determined in order to keep PTOT to the imposed value. The final properties of the gas mixture in SIMMER-IV are eventually calculated according to PVAP, PINC and TGAS.

Regarding the mass flow rate, it is important to clarify that in SIMMER-IV the incondensable gas and all the vapours (steam in this case) share the same velocity field as a single multicomponent gas mixture but, notably, a diffusion coefficient is calculated for each component individually.

## 2. Coupled simulations

### 2.1. LIFUS5/Mod3 experimental campaign

LIFUS5/Mod3 is an experimental facility designed and developed at the ENEA Brasimone Research Centre (Italy). The aim of the facility is to investigate the physical and chemical interaction of water and PbLi alloy. A simplified scheme of the facility is presented in Fig. 4a: it consists of an injection line partially filled with water and Argon, and a reaction tank (S1B) in which the heavy liquid metal is contained. The geometrical volume of the S1B vessel is about 30 L and during the experiments is filled with Lead-Lithium alloy and covered with Argon at about 0.2 barg. The water injection line penetrates into the S1B vessel from the bottom, aligned with its axis; in this way an axial-symmetric configuration is obtained, in order to facilitate the nodalization of the domain in the SIMMER-codes. The injection line and the S1B tank are initially isolated by means of an injector covered sealed by a cap, installed at the exit of the injection line (in the S1B tank). The tank is initially at atmospheric pressure, while the injection line is at a higher pressure. One of the main tasks of the LIFUS5/Mod3 experimental campaign is to validate the application of the SIMMER-IV code for the prediction of PbLi-water interaction and to improve and verify the reliability of the coupling methodology between SIMMER-IV and RELAP5 presented here.

Fig. 4b and c show the test section inserted into the vessel S1B. This component is welded directly on the top flange of S1B and is designed to be axial-symmetric. The upper holed plate, visible on the left part of Fig. 4b, delimits the interaction zone where the chemical reaction can

take place, by breaking down the impinging jet of subcooled water from the injector. Simultaneously, the holes allow the passage of water vapour and hydrogen produced during the tests.

The lateral sides of the test section are instead open, to allow the propagation of the pressure wave generated during the interaction and its measurement through the sensors positioned on the sides of the vessel. These sensors include both strain gages and dynamic pressure transducers, to record the vessel deformation and pressure wave intensity and shape. A total of 74 0.5 mm K-type thermocouples are installed on the test section, over six different levels ranging in elevation from the injector to the holed plate, and uniformly distributed in the radial direction (Fig. 4c).

Two main experimental series were conducted in L5M3, namely SERIES D and E. In both series the tests were conducted with the same general procedure: the injection line was partially filled with subcooled water and then connected to a tank containing pressurised Argon; once the connection is established, the pressure in the line started increasing rapidly, until the cap which separates the line and the S1B vessel breaks abruptly, and a mixture of Argon and water is injected inside the vessel. Several tests were run, varying a number of initial characteristics, in order to analyse the effects of these changes on the behaviour of the main thermodynamic parameters. The test matrixes of the two series are reported in Tables 1 and 2.

The main difference between the two series is the amount of water injected during the transient. In series D the mass of water is pre-determined and relatively small (varying from 50 to 150 gs) whilst in series E the water is injected continuously for a pre-fixed interval of time and then the total mass of injected water is estimated a posteriori (reaching up to 400 gs of water).

#### 2.1.1. Coupled nodalizations

In the coupled simulations, the S1B vessel and the last part of the injection line are simulated by SIMMER-IV, whilst the remainder of the injection line by RELAP5.

In the RELAP5 nodalization the injection line is fully nodalized, reproducing all the main features of the line, including the Coriolis section (Fig. 5). The nodalization consists of volume elements, with a specified area and length. The different volume elements and their properties are listed in Table 3 and shown in Fig. 5. The volume elements are connected to each other using junctions, to which a pressure drop coefficient can be assigned. The junctions are used here to reproduce the change of orientation of the pipes. The injection line starts with SBL, which is modelled as a pipe with 28 volume elements. The water tank is pressurized by a time dependent volume, representing the argon tank. They are connected by a single junction. The bottom of SBL is connected

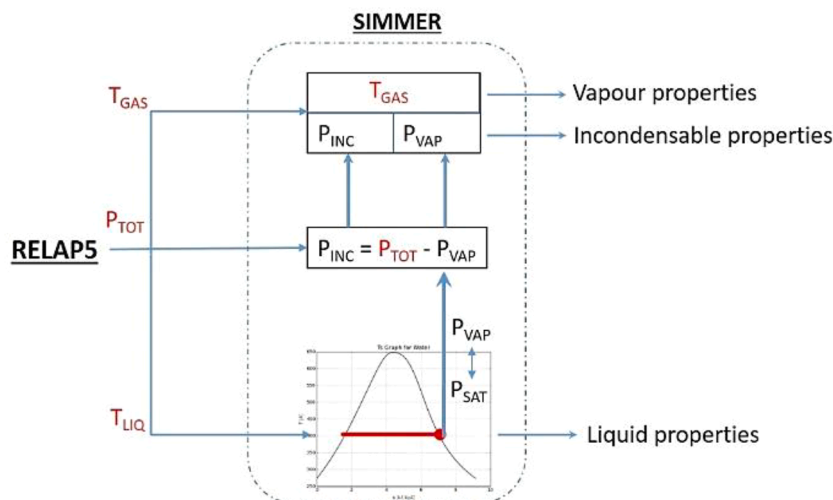


Fig. 3. Multiphase properties coupling scheme.

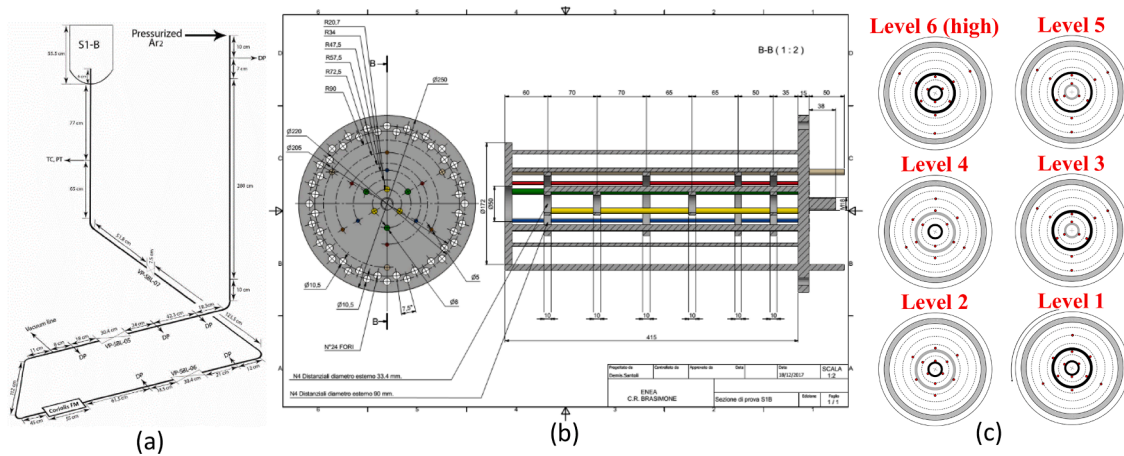


Fig. 4. Details of LIFUS5/M3 facility: (a) Schematic drawings of the injection line; (b) Schematic drawing of the test section; (c) Layout implementation of the thermocouples.

Table 1  
Series D test matrix.

Test Series	Mass of water [g]	Water T [°C]	PbLi T [°C]	Injection Pressure [bar]
D	50	295	330	155
#1	50	295	330	155
#2	50	330	330	155
#3	50	295	450	155
#4	100	295	330	155
#5	150	295	330	155

Table 2  
Series E test matrix.

Test Series	D orifice [mm]	Water T [°C]	PbLi T [°C]	Injection Time [s]	Injection pressure [bar]
E	4	295	330	1	155
#1	4	295	430	1	155
#2	1	295	330	0.5	155
#3	2	295	330	1	155
#4	1	295	330	1.5	155
#5	4	295	380	1	155
#6	2	295	380	1.3	155
#7	1	295	380	2	155
#8	1	295	380	2	155

via a single junction to a smaller pipe containing 10 volume elements. This pipe is connected to a motor valve representing VP-SBL-05. The valve can be opened or closed, and it is also possible to assign the timing of action. A valve is only a junction, so the volume elements of this valve are incorporated into the next and previous pipe. After other four pipes, two motor valves, representing VP-SBL-06 and VP-SBL-07 and a junction, the line is connected to a trip valve.

In order to test the coupling technique different nodalizations of the S1B were created. Since the scope of this work is to develop and test the methodology, for the sake of brevity only two versions of the mesh are presented here: one extremely rough mesh, composed by only 512 cells, whilst another one significantly more refined with 40,500 cells. However, the coupling was tested successfully also with other versions of the mesh. The simplified mesh is shown in Figs. 6, 7 and 8 and it is composed of 8 cells in both x and y directions (respectively called I and K dimensions in SIMMER) and by 8 cells in the vertical direction (z, or J in SIMMER). The red region from cells  $J = 4$  to  $7$  represents the S1B volume filled with liquid lead-lithium and covered by Argon on cell  $J = 8$ . The injection line region goes from I and K equal 3 to 6 and  $J = 1-5$ , with cells 4 and 5 representing the penetration of the injection line inside the S1B.

The refined mesh is shown in Fig. 9. In this nodalization all the main geometrical characteristics and main parts of the S1B are represented. First of all, in Fig. 9 it is possible to distinguish the tip of the injection line, at the bottom of the mesh. Secondly, the hemispherical base of the vessel was created, using ten layers of vertical cells. Furthermore, all the

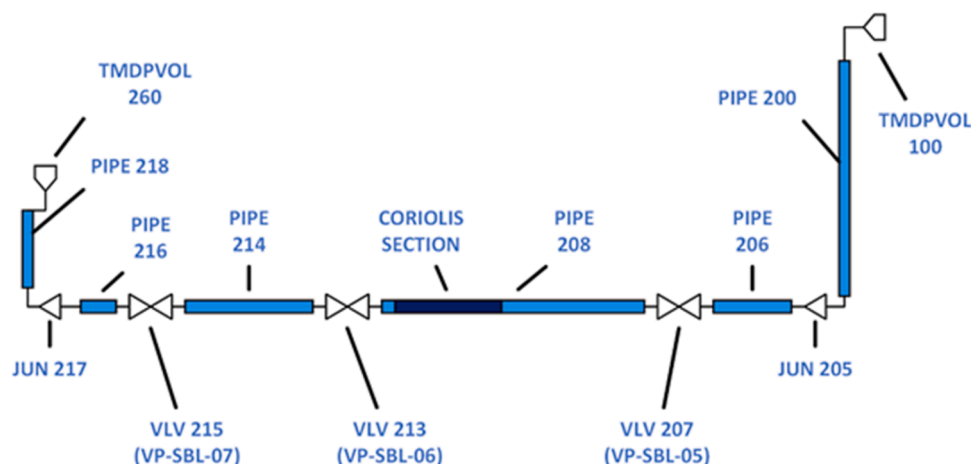


Fig. 5. RELAP5/Mod3.3 nodalization of the injection line (only pipes length on scale).

**Table 3**  
Characteristics of RELAP5/Mod3.3 nodalization.

Component number	Hydrodynamic component	Description	Length [m]	Area [m <sup>2</sup> ]
100	Time dependent volume	Argon tank	[-]	[-]
200	Pipe	SBL	2.8	9.069e-04
205	Single junction		[-]	
206	Pipe		1.096	6.936e-05
207	Motor valve	VP-SBL-05	[-]	6.93e-05
208	Pipe	Normal section	2.094	6.936e-05
		Coriolis section	1.48	6.12e-04
213	Motor valve	VP-SBL-06	[-]	6.93e-05
214	Pipe		1.742	6.936e-05
215	Motor valve	VP-SBL-07	[-]	6.93e-05
216	Pipe		0.518	6.936e-05
217	Single junction		[-]	
218	Pipe		1.4	6.936e-05
260	Time dependent volume	Coupling interface	[-]	[-]

most important components of the test section were generated, together with the perforated upper plate which separates the lead-lithium from the cover gas; the solid parts were modelled in SIMMER-IV as steel.

Although both the nodalizations tried to remain as close as possible to the real dimensions of the S1B vessel, even the refined computational domain still retains some level of inaccuracy; however, it is important to notice that the aim at this stage of the work is not to accurately reproduce the experiments, but instead to evaluate and assess the performances of the coupling. On the other hand, the nodalization of the injection line closely matches the geometrical characteristics of the real facility.

The coupling scheme between the two domains is shown in Fig. 10. The boundary conditions are coupled through TMDPVOL260 in the RELAP5 domain and the surfaces related to the injection line in the SIMMER-IV domain.

The main cases selected to test the coupling for full simulations were two, namely D15 from series D and E41 from series E. These two cases

allowed us to perform simulations using initial and boundary conditions from real experimental tests. Furthermore, the two cases differ in the way the water is injected, with a fast injection for the D case and a prolonged injection for the E case and this is a further important proofing ground for the multiphase coupling. Table 4 summarizes the main characteristics of the selected cases.

**2.1.2. Boundary and initial conditions**

The reference calculation starts at  $t = 0$  s and the two domains are let run in stationary boundary conditions for 1 s, in order to allow the coupled cells to perfectly synchronise on the initial conditions; after 1 s the transient simulation starts opening RELAP5 component VLV 213, which represents the valve VP-SBL-06 opening in the experiment. The injector cap rupture is simulated by the disappearance of the SIMMER-IV virtual walls on the top of the injection line, which recreate the orifice of the injector. The time at which the injector cap breaks up is obtained from the specific test experimental data.

Regarding the BC set-up pressure and temperature, the experimental recording obtained from the specific probes closest to the Argon gas tank (i.e., PC-SBL-01 and TC-SBL-01) were imposed as timetables in RELAP5 at TMPVOL 100. The initial conditions for the thermodynamic properties of the fluids in S1B and the amount of water are set coherently with the experimental data reported in Table 4.

**3. Results**

**3.1. Coupling synchronisation and accuracy**

Since this work is devoted to the development of a coupling technique between two significantly different codes in a complex multiphase scenario, which involves the exchange and the calculation of the properties and thermodynamic state of a mixture of water in liquid and vapour phases and an incondensable gas (Argon), the very first aim must be to obtain a close match between the thermodynamic variables calculated in the cells at the interface of the two domains.

The post-processing and visualization of the data were carried out with MATLAB and Paraview [28] software packages.

Figs. 11–19 show the time evolution of the variables that are monitored to check the quality of the coupling for the coarse mesh. It is quite clear that the two computational domains are thoroughly coupled.

Figs. 11, 12 and 13 present the coupled pressure. The two pressures are perfectly matched for all the cases, both for the coarse and the

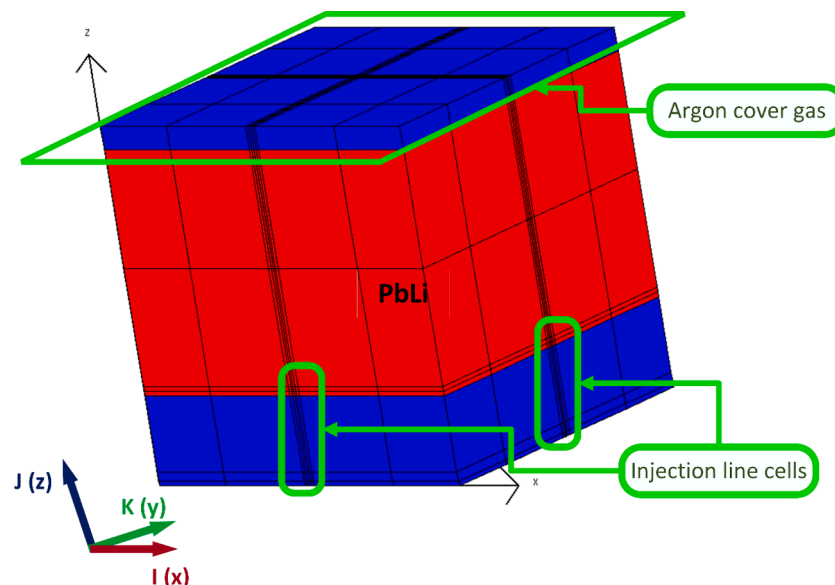


**Fig. 6.** SIMMER-IV coarse mesh - 3D visualization.

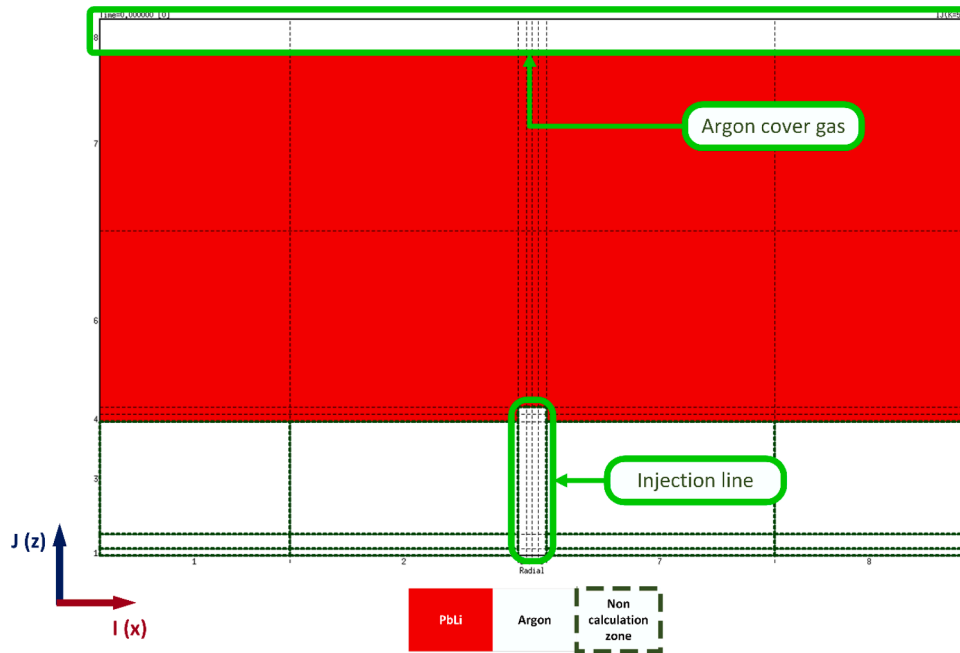


Fig. 7. SIMMER-IV coarse nodalization - IJ plane,  $K = 5$  - The size of the cells is shown on a real scale.

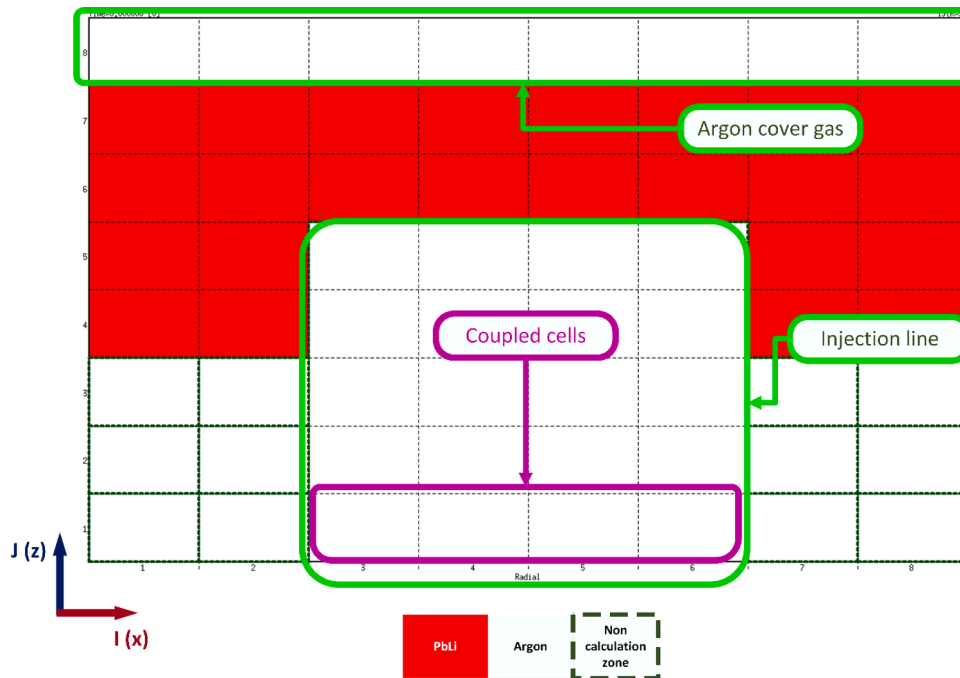


Fig. 8. SIMMER-IV coarse nodalization - IJ plane,  $K = 5$  - The size of the cells is shown on an even scale.

refined mesh.

Figs. 14–16, show the coupled mass flow rate for the gas mixture (i. e., Argon and steam). This coupling presents some discrepancies in the E41 case. Considering the single mass flow rate of the steam, it is clear that the significant difference is due to the fraction of steam transferred between the boundaries (Figs. 17–19); it is interesting to notice that this discrepancy is quite relevant for the case with the refined mesh. Nevertheless, since the steam flow rate remains nearly always well below 10% of the total mass flow rate, this difference is considered negligible at this stage, but it will be the subject of further improvement. Fig. 15, Fig. 18, Fig. 21.

Figs. 20–22 show the coupled liquid mass flow rate. Also for this variable the coupling is remarkably good for all the cases, and the coupling remains stable for the two different kinds of water injections. Overall, the quality of the coupling can be considered excellent.

### 3.2. Preliminary qualitative results

In order to provide a first evaluation of the capabilities and strengths of using SIMMER-IV, some examples of the possible outputs are reported in this section, with figures obtained from the simulation of E41 case realised with the refined mesh. The rupture time and, therefore, the

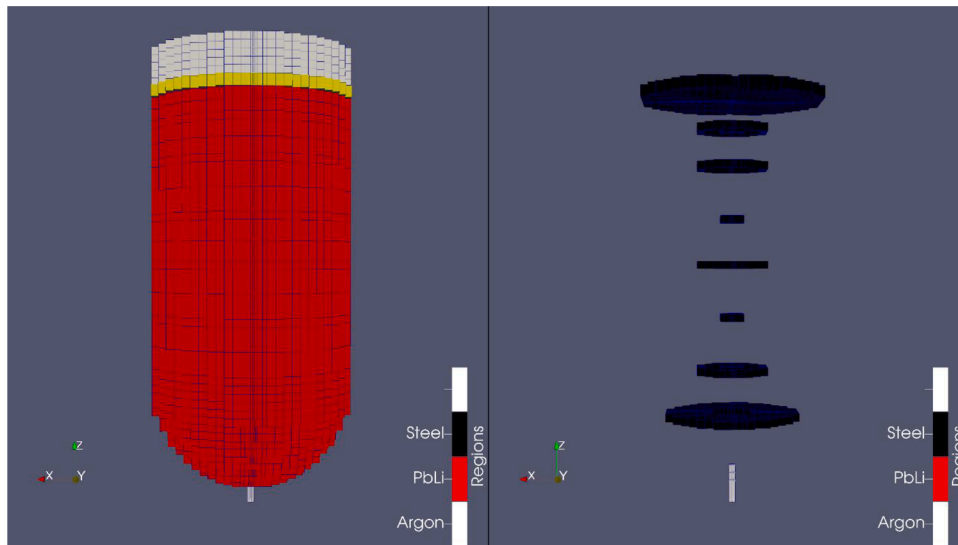


Fig. 9. Refined SIMMER-IV mesh for S1B.

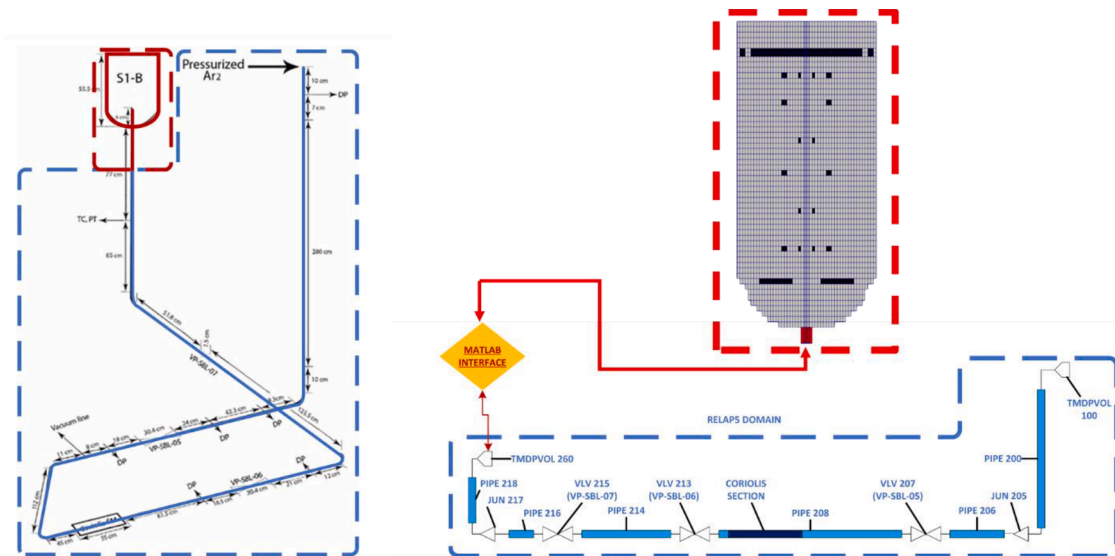


Fig. 10. SIMMER-IV/RELAP5 coupling scheme of LIFUS5/Mod3 injection line and S1B vessel.

Table 4  
Parameters of simulation test cases.

Test Series	Case number	D orifice [mm]	Mass of water [g]	Injection Time [s]	Water T [ °C]	PbLi T [ °C]	Injection Pressure [bar]
D	1.5	4	50	–	295	330	155
E	4.1	2	–	1	295	330	155

beginning of the water injection is at 1.229 s. Figs. 23–25 show six snapshots of the distribution of different parameters at six different instants in time. The snapshots were obtained through a zx plane placed at the centre of the computational domain. Fig. 26 presents four snapshots of an xy plane at four different heights of the S1B. The figures are described and briefly commented below; however, it is important to remark that these results are presented here only as an example and by no means they represent an attempt of code validation. For this reason, no comparison with experimental data is reported.

Fig. 23 presents the distribution of different fluids in the vessel and in the last part of the injection line. The computational domain starts with only Argon and lead-lithium with the incondensable gas filling the

injection line and the upper part of the vessel, above the perforated plate. Immediately before the rupture, the injection line is partially occupied by pressurised water, which strongly compresses the gas against the cap. After the rupture of the cap, a mixture of steam, Argon and liquid water is abruptly injected inside the vessel and pushes the lead-lithium through the perforated plate. Afterwards, an intermittent jet of liquid water is formed inside the S1B. The water interacts with the lead-lithium forming lithium oxide (Li<sub>2</sub>O); it must be clarified that, in Fig. 23, in order to obtain a better visualisation of the volume fraction scale of the Li<sub>2</sub>O is extremely exaggerated (it is actually multiplied by 10). After a while, the gas mixture tends to accumulate again in the upper part of the S1B.



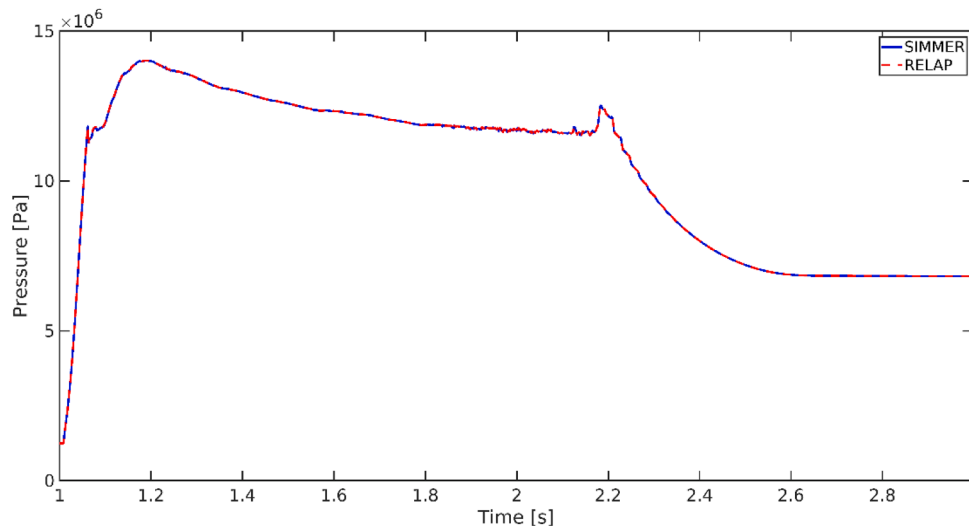


Fig. 11. Coarse mesh - Coupling quality monitoring for D15 case – Coupled pressure.

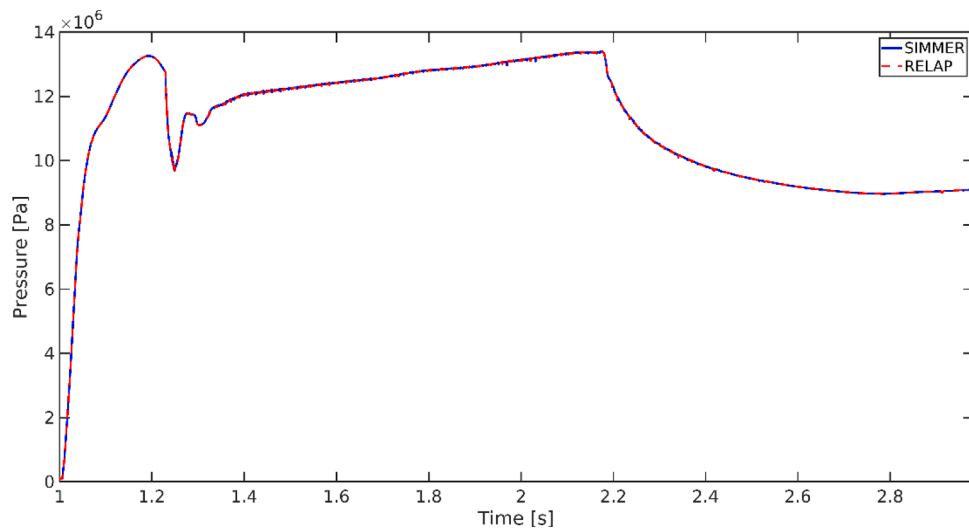


Fig. 12. Coarse mesh - Coupling quality monitoring for E41 case – Coupled pressure.

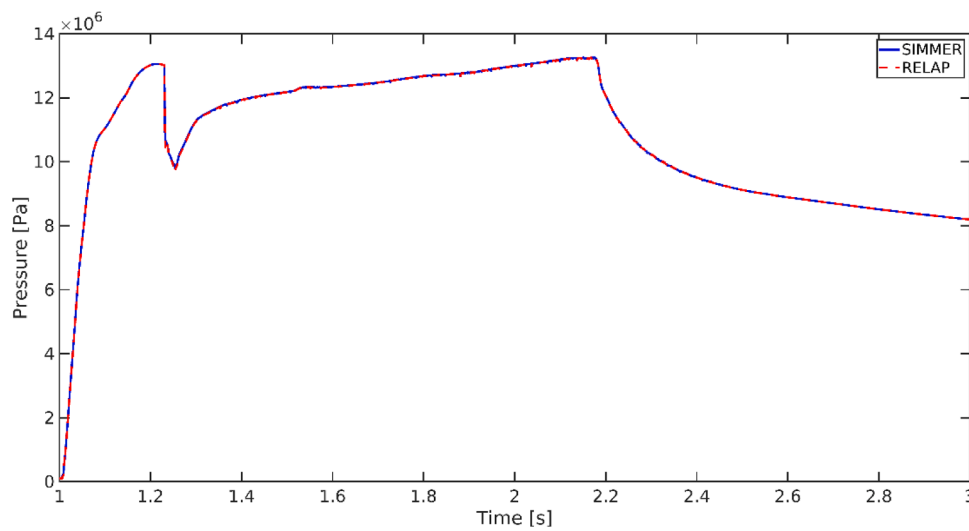


Fig. 13. Refined mesh - Coupling quality monitoring for E41 case – Coupled pressure.

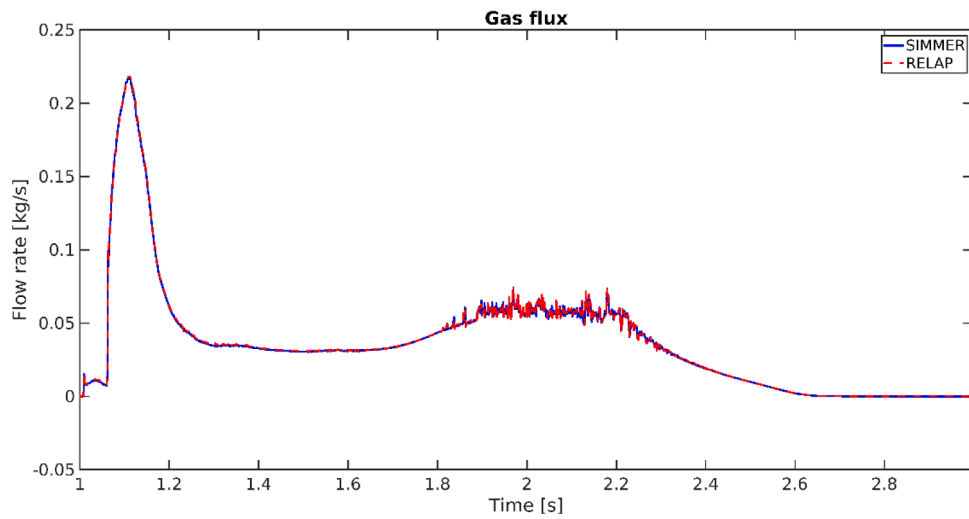


Fig. 14. Coarse mesh - Coupling quality monitoring for D15 case – Coupled gas flow rate.

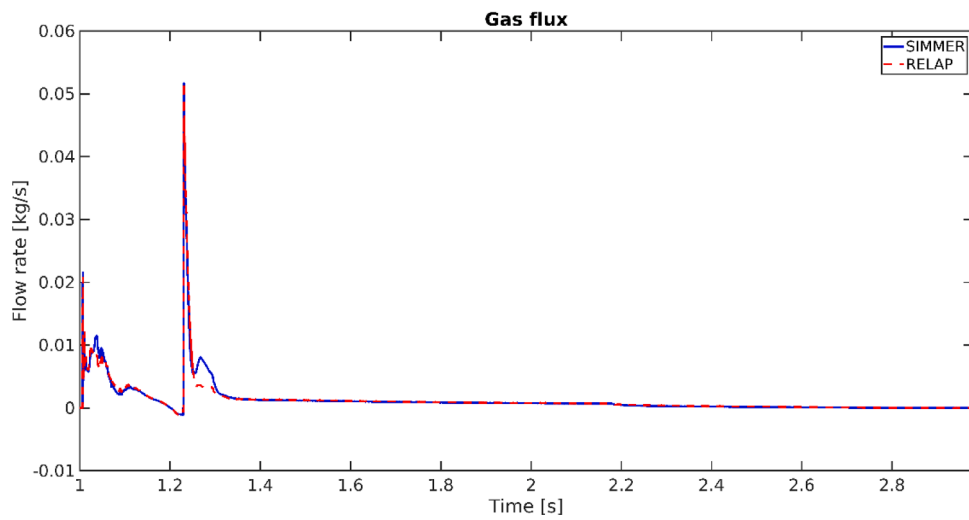


Fig. 15. Coarse mesh - Coupling quality monitoring for E41 case – Coupled gas flow rate.

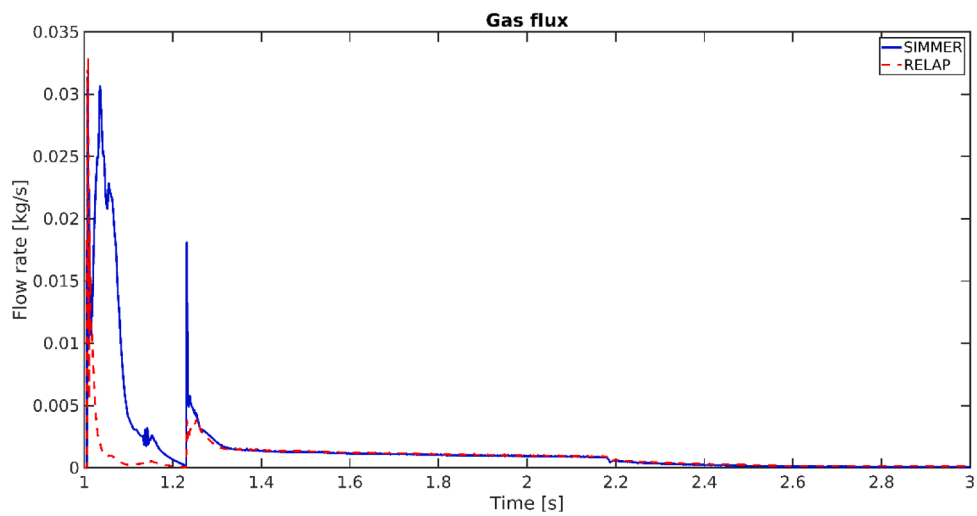


Fig. 16. Refined mesh - Coupling quality monitoring for E41 case – Coupled gas flow rate.

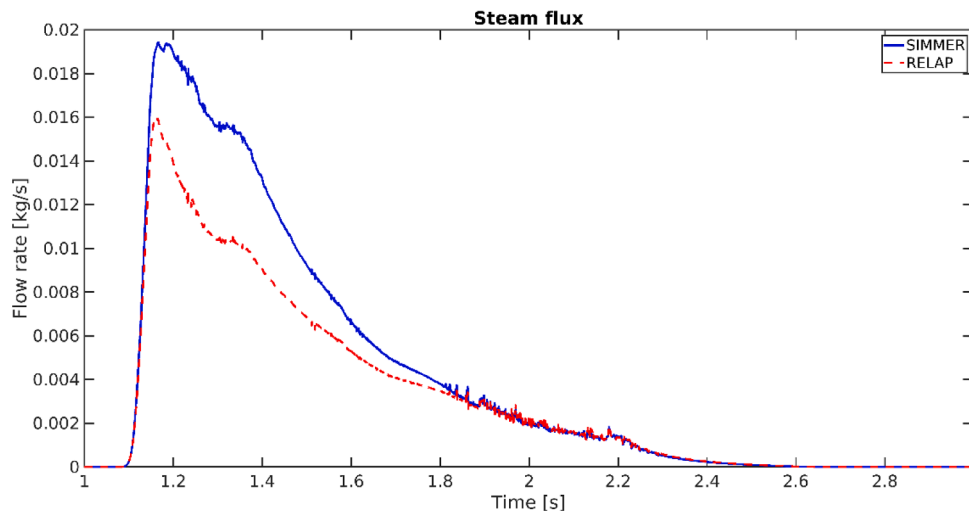


Fig. 17. Coarse mesh - Coupling quality monitoring for D15 case – Coupled steam flow rate.

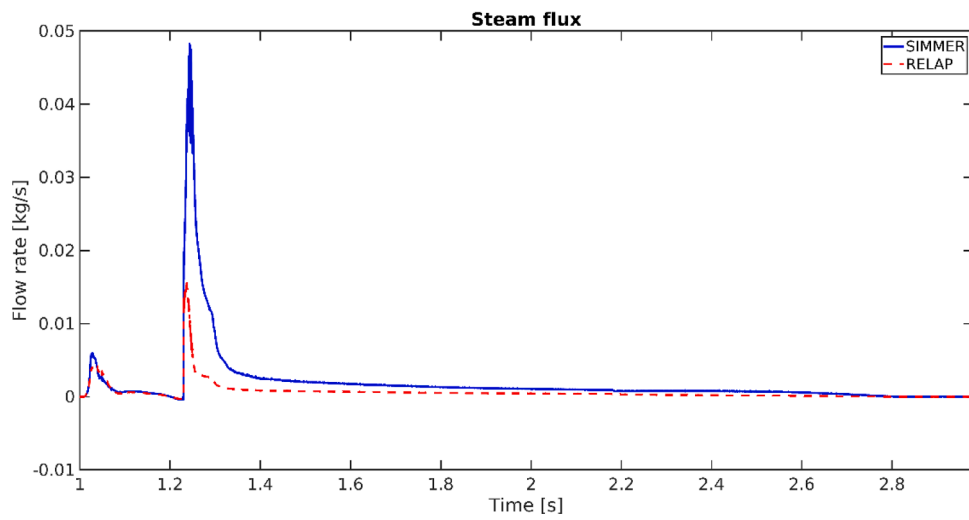


Fig. 18. Coarse mesh - Coupling quality monitoring for E41 case – Coupled steam flow rate.

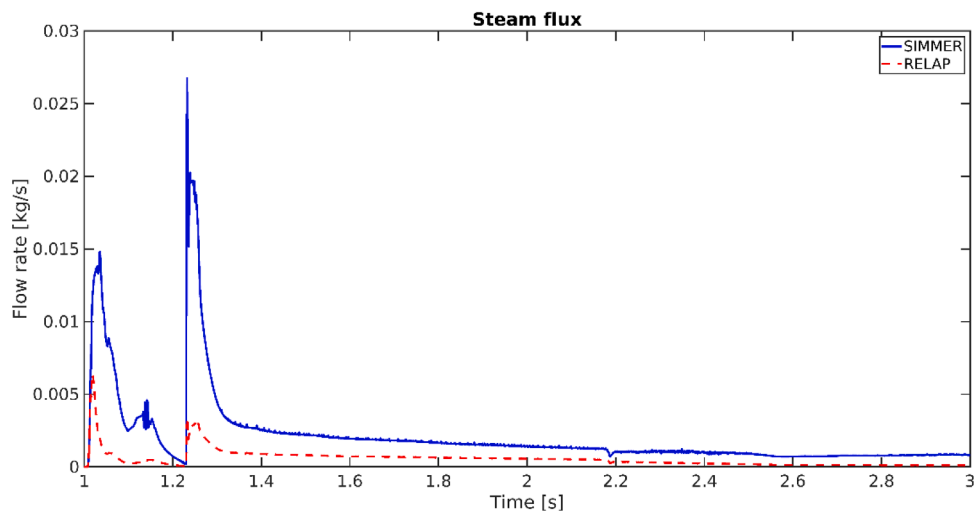


Fig. 19. Refined mesh - Coupling quality monitoring for E41 case – Coupled steam flow rate.

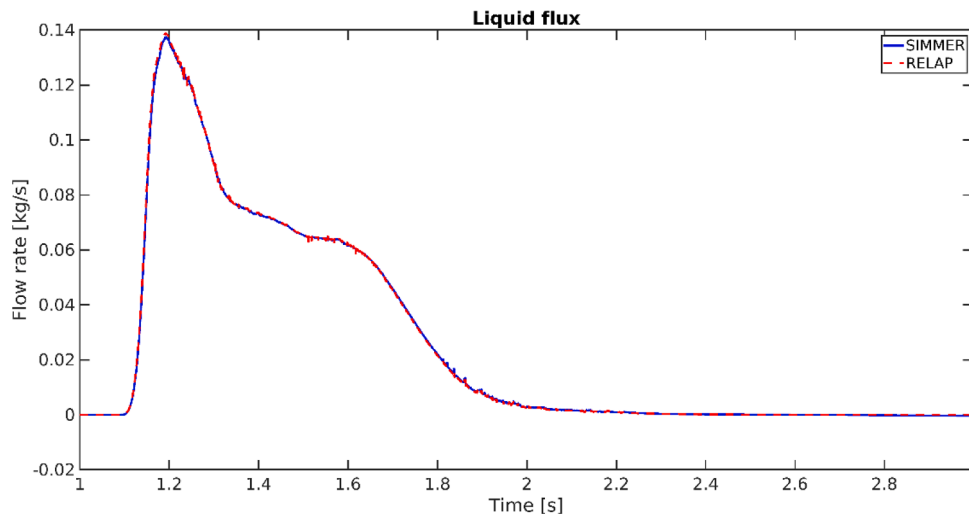


Fig. 20. Coarse mesh - Coupling quality monitoring for D15 case – Coupled liquid flow rate.

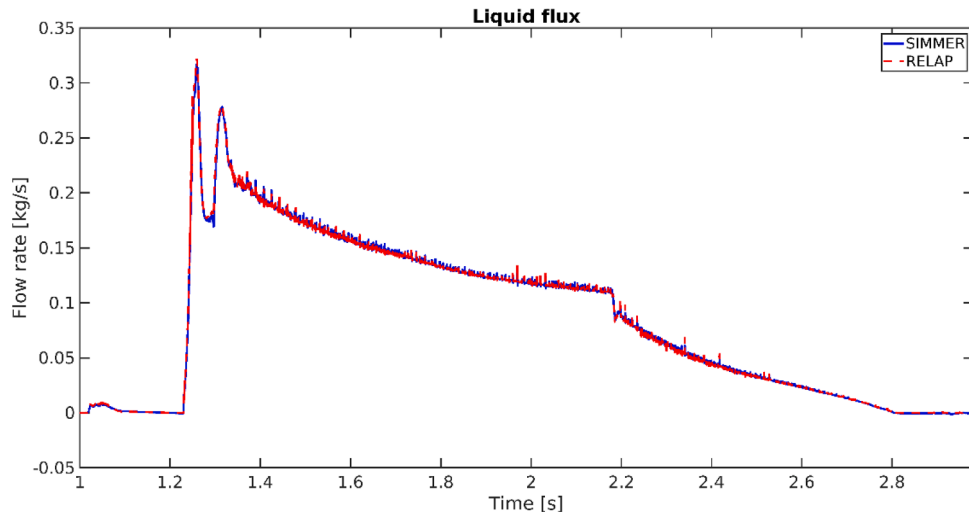


Fig. 21. Coarse mesh - Coupling quality monitoring for E41 case – Coupled liquid flow rate.

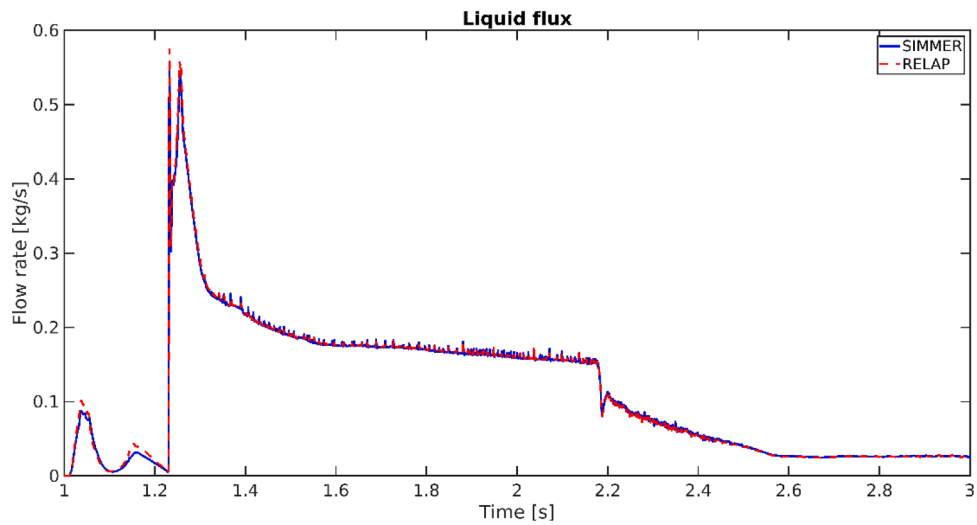


Fig. 22. Refined mesh - Coupling quality monitoring for E41 case – Coupled liquid flow rate.

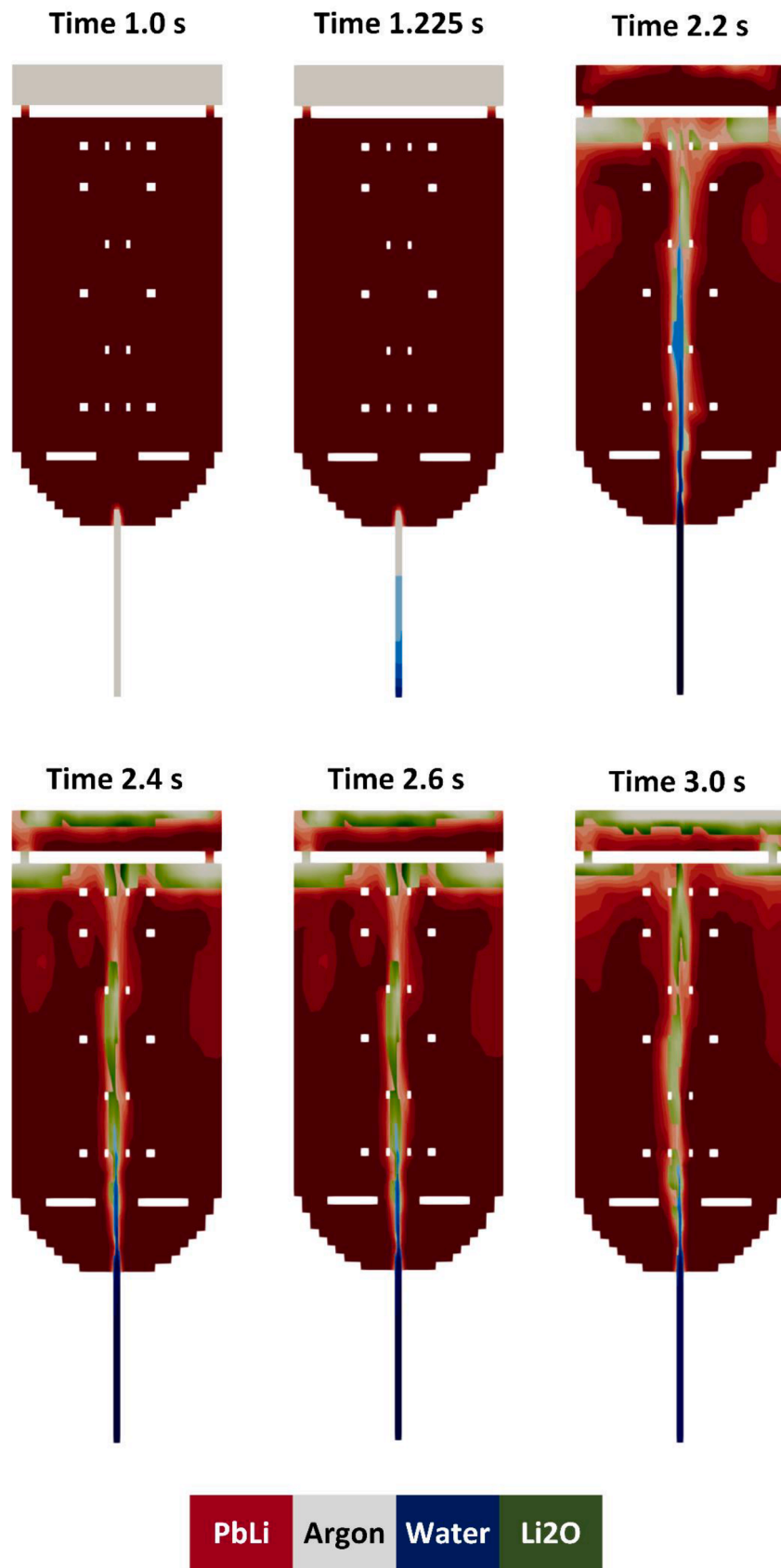


Fig. 23. Time snapshots of volume fraction distribution in S1B for case E41 (exaggerated scale for Li2O).



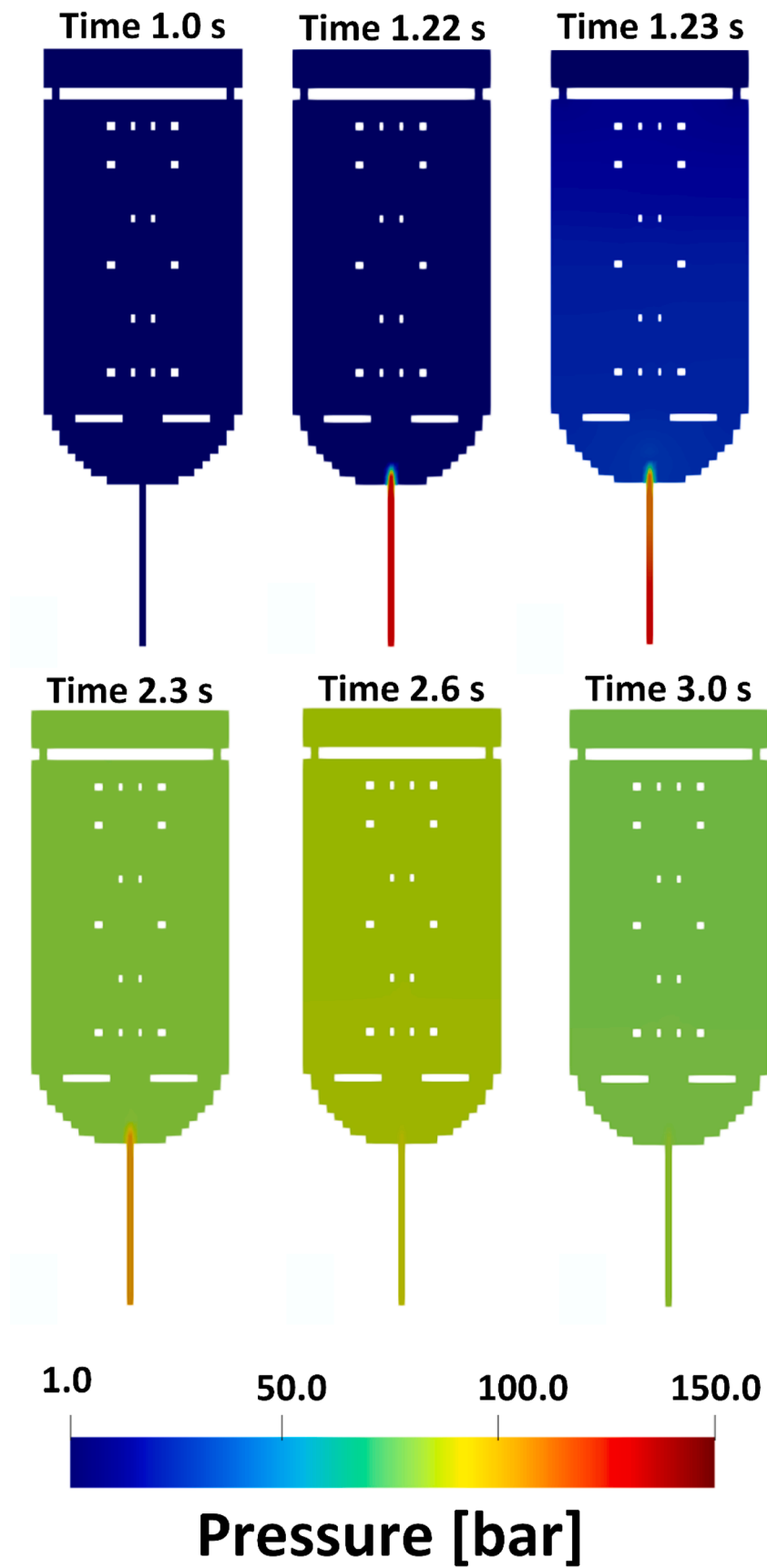


Fig. 24. Time snapshots of pressure distribution in S1B for case E41.

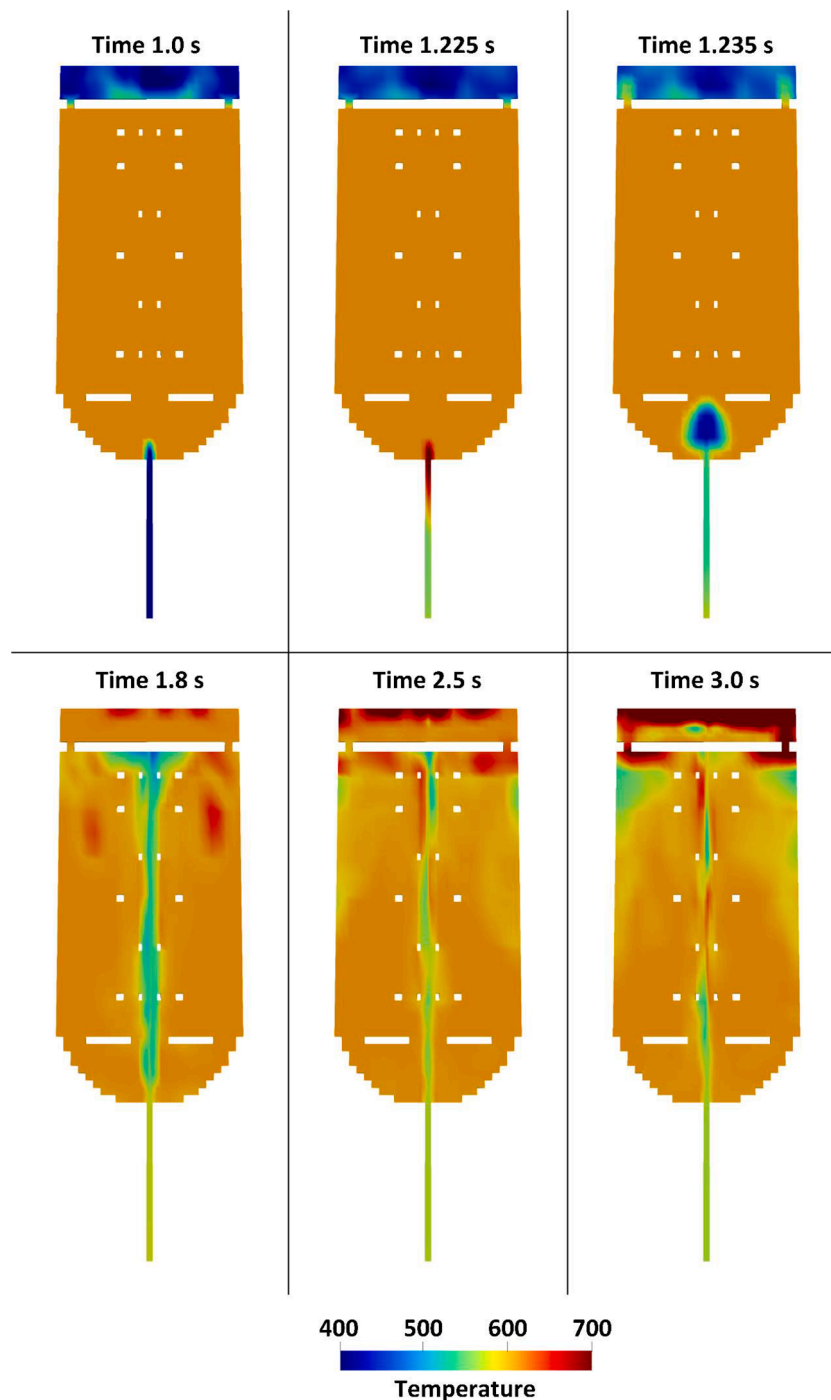


Fig. 25. Time snapshots of average temperature distribution in S1B for case E41.

Fig. 24 shows the pressure distribution in the S1B. It is interesting to see that, at least at this time scale, the pressure seems to remain essentially homogenous in the S1B throughout all the transient, the only exception being the instant immediately after the rupture, which shows a weak axial pressure gradient.

Fig. 25 shows the average temperature (weighted by the volume fraction) in the S1B. It is noteworthy to notice that the highest contribution to the average temperature is given by the incondensable gas.

#### 4. Conclusions

This paper summarises the progress made in the development of a numerical multi-physics coupled tool for safety analysis of fusion

reactors and related experimental facilities in relevant operative conditions. This coupled tool is based on the coupling between the two versions of SIMMER code (namely SIMMER-III and SIMMER-IV, 2D and 3D codes respectively) and the one-dimensional STH code RELAP5.

In particular, the work presented here involved the development and testing of the extension of the coupling technique to SIMMER-IV and RELAP5. The main characteristics of the coupling were explained and several test cases – derived from real experimental campaigns – were presented.

The results show the successful application of this extension of the coupling to SIMMER-IV and the testing of the coupling with complex simulations. The coupling proved to be effective and robust, already reproducing the complex behaviour of the real experimental boundary

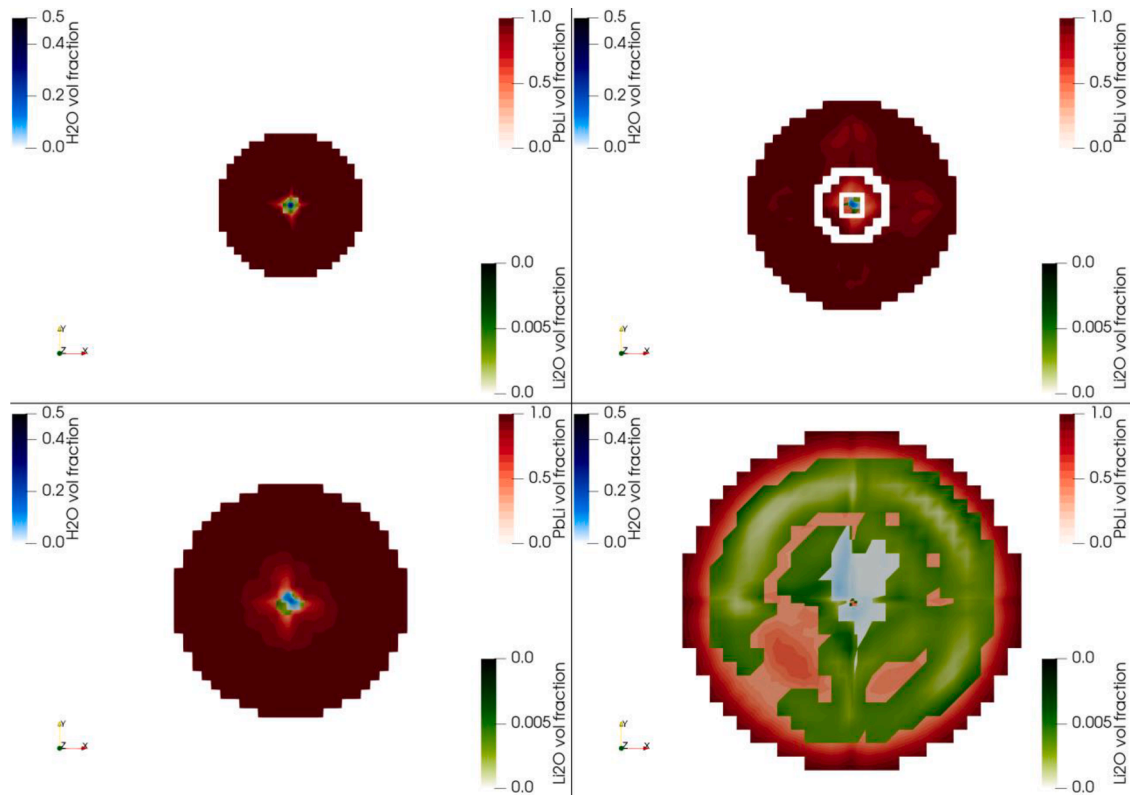


Fig. 26. Volume fraction distribution in S1B for case E41 at different heights and time 2.6 s (exaggerated scale for Li2O).

conditions exchanged through the two computational domains.

In terms of the general background of this work, compared to SIMMER-III, SIMMER-IV presents the only shortcoming of a considerably longer computational time required for long simulations. This is due to the significant increase of cells switching from a 2D to a 3D domain but also strongly to the fact that S-IV is not parallelised, whilst S-III is. This remains an issue that should not be overlooked, especially with the final objective of developing a flexible code for safety analysis.

However, the capability of SIMMER-IV of simulating three-dimensional domains remains an invaluable step forward, considering the complexity of the involved geometries for the various WCLL configurations and components.

#### Declaration of Competing Interest

The authors declare that they have no known competing financial interests or personal relationships that could have appeared to influence the work reported in this paper.

#### Data availability

The data that has been used is confidential.

#### Acknowledgments

This work has been carried out within the framework of the EUROfusion Consortium, funded by the European Union via the Euratom Research and Training Programme (Grant Agreement No 101052200 — EUROfusion). Views and opinions expressed are however those of the author(s) only and do not necessarily reflect those of the European Union or the European Commission. Neither the European Union nor the European Commission can be held responsible for them.

#### References

- [1] F.S. D'Auria et al., 'Neutronics/thermal-hydraulics coupling in LWR technology—CRISSUE-S', 2004.
- [2] O. Zerkak, T. Kozłowski, I. Gajev, Review of multi-physics temporal coupling methods for analysis of nuclear reactors, *Ann. Nucl. Energy* 84 (2015) 225–233, <https://doi.org/10.1016/j.anucene.2015.01.019>. Oct.
- [3] J. Long, B. Zhang, B.-W. Yang, S. Wang, Review of researches on coupled system and CFD codes, *Nucl. Eng. Technol.* 53 (9) (2021) 2775–2787, <https://doi.org/10.1016/j.net.2021.03.027>. Sep.
- [4] J. Wang, Q. Wang, M. Ding, Review on neutronic/thermal-hydraulic coupling simulation methods for nuclear reactor analysis, *Ann. Nucl. Energy* 137 (2020), 107165, <https://doi.org/10.1016/j.anucene.2019.107165>. Mar.
- [5] A. Pucciarelli, et al., Coupled system thermal Hydraulics/CFD models: general guidelines and applications to heavy liquid metals, *Ann. Nucl. Energy* 153 (2021), 107990, <https://doi.org/10.1016/j.anucene.2020.107990>.
- [6] G. Federici, et al., DEMO design activity in Europe: progress and updates, *Fusion Eng. Des.* 136 (2018) 729–741.
- [7] L. Boccaccini, et al., Status of maturation of critical technologies and systems design: breeding blanket, *Fusion Eng. Des.* 179 (2022), 113116.
- [8] P. Arena, et al., The DEMO water-cooled lead–lithium breeding blanket: design status at the end of the pre-conceptual design phase, *Appl. Sci.* 11 (24) (2021), <https://doi.org/10.3390/app112411592>, 24ArtJan.
- [9] G. Caruso, et al., DEMO – The main achievements of the Pre – Concept phase of the safety and environmental work package and the development of the GSSR, *Fusion Eng. Des.* 176 (2022), 113025, <https://doi.org/10.1016/j.fusengdes.2022.113025>. Mar.
- [10] D.W. Jeppson, L.D. Munlestein, Safety considerations of lithium lead alloy as a fusion reactor breeding material, *Fusion Technol.* 8 (1) (1985) 1385–1391, <https://doi.org/10.13182/fst85-a39960>, pt 2(B).
- [11] H. Kottowski, O. Kranert, C. Savatter, C. Wu, M. Corradini, Studies with respect to the estimation of liquid metal blanket safety, *Fusion Eng. Des.* 14 (3–4) (1991) 445–458, [https://doi.org/10.1016/0920-3796\(91\)90024-K](https://doi.org/10.1016/0920-3796(91)90024-K).
- [12] S.J. Piet, D.W. Jeppson, L.D. Muhlestein, M.S. Kazimi, M.L. Corradini, Liquid metal chemical reaction safety in fusion facilities, *Fusion Eng. Des.* 5 (3) (1987) 273–298, [https://doi.org/10.1016/S0920-3796\(87\)90032-9](https://doi.org/10.1016/S0920-3796(87)90032-9).
- [13] M. Eboli, A. Del Nevo, A. Pesetti, N. Forgiione, P. Sardain, Simulation study of pressure trends in the case of loss of coolant accident in Water Cooled Lithium Lead blanket module, *Fusion Eng. Des.* 98–99 (2015) 1763–1766, <https://doi.org/10.1016/j.fusengdes.2015.05.034>.
- [14] A. Tincani, et al., Conceptual design of the main ancillary systems of the ITER water cooled lithium lead test blanket system, *Fusion Eng. Des.* 167 (2021), 112345, <https://doi.org/10.1016/j.fusengdes.2021.112345>. Jun.

- [15] G.A. Spagnuolo, et al., Integrated design of breeding blanket and ancillary systems related to the use of helium or water as a coolant and impact on the overall plant design, *Fusion Eng. Des.* 173 (2021), 112933, <https://doi.org/10.1016/j.fusengdes.2021.112933>. Dec.
- [16] R. Mozzillo, M. Utili, A. Venturini, A. Tincani, C. Gliss, Integration of LiPb loops for WCLL BB of European DEMO, *Fusion Eng. Des.* 167 (2021), 112379, <https://doi.org/10.1016/j.fusengdes.2021.112379>. Jun.
- [17] B. Gonfiotti, S.K. Moghanaki, M. Eboli, G. Barone, A. Del Nevo, D. Martelli, Development of a SIMMER\RELAP5 coupling tool, *Fusion Eng. Des.* 146 (2019) 1993–1997, <https://doi.org/10.1016/j.fusengdes.2019.03.084>. Sep.
- [18] F. Galleni, et al., RELAP5/SIMMER-III code coupling development for PbLi-water interaction, *Fusion Eng. Des.* 153 (2020), 111504, <https://doi.org/10.1016/j.fusengdes.2020.111504>.
- [19] 'SIMMER-III: A computer program for LMFR Core disruptive accident analysis', O-arai Engineering Center - Japan Nuclear Cycle Development Institute, JNC TN 9400 2003–071, Aug. 2003.
- [20] 'SIMMER-IV: A three-dimensional computer program for LMFR core disruptive accident analysis', O-arai Engineering Center - Japan Nuclear Cycle Development Institute, JNC TN 9400 2003–070, Aug. 2003.
- [21] Information Systems Laboratories, Inc., 'RELAP5/MOD3.3 Code Manual Volume I: Code Structure, System Models, And Solution Methods', Division of Systems Analysis Office of Nuclear Regulatory Research - U. S. Nuclear Regulatory Commission, Rockville, Maryland - Idaho Falls, Idaho - United States, 2019. NUREG/CR-5535/Rev P5-Vol I Feb.
- [22] M. Eboli, N. Forgione, A. Del Nevo, Implementation of the chemical PbLi/water reaction in the SIMMER code, *Fusion Eng. Des.* 109–111 (2016) 468–473, <https://doi.org/10.1016/j.fusengdes.2016.02.080>. Nov.
- [23] 'MATLAB version 9.12 (R2022a)'. The Mathworks, Inc., Natick, Massachusetts, 2022.
- [24] M. Eboli, S.K. Moghanaki, D. Martelli, N. Forgione, M.T. Porfiri, A. Del Nevo, Experimental activities for in-box LOCA of WCLL BB in LIFUS5/Mod3 facility, *Fusion Eng. Des.* 146 (2019) 914–919, <https://doi.org/10.1016/j.fusengdes.2019.01.113>. Sep.
- [25] M. Eboli, R.M. Crugnola, A. Cammi, S. Khani, N. Forgione, A. Del Nevo, Test Series D experimental results for SIMMER code validation of WCLL BB in-box LOCA in LIFUS5/Mod3 facility, *Fusion Eng. Des.* 156 (2020), 111582, <https://doi.org/10.1016/j.fusengdes.2020.111582>. Jul.
- [26] M. Eboli, F. Galleni, N. Forgione, N. Badodi, A. Cammi, A. Del Nevo, Experimental and numerical results of LIFUS5/Mod3 series E Test on In-Box LOCA transient for WCLL-BB, *Energies* 14 (24) (2021) 8527, <https://doi.org/10.3390/en14248527>.
- [27] S. Khani Moghanaki, F. Galleni, M. Eboli, A.D. Nevo, S. Paci, N. Forgione, Analysis of Test D1.1 of the LIFUS5/Mod3 facility for In-box LOCA in WCLL-BB, *Fusion Eng. Des.* 160 (2020), 111832, <https://doi.org/10.1016/j.fusengdes.2020.111832>. Nov.
- [28] J. Ahrens, B. Geveci, C. Law, Paraview: an end-user tool for large data visualization, *Los Alamos Natl. Lab. Tech. Rep.* 717 (8) (2005).